

# Making metallic glasses plastic by control of residual stress

Y. ZHANG<sup>1</sup>, W. H. WANG<sup>2</sup> AND A. L. GREER<sup>1\*</sup>

<sup>1</sup>Department of Materials Science & Metallurgy, University of Cambridge, Pembroke Street, Cambridge CB2 3QZ, UK

<sup>2</sup>Institute of Physics, Chinese Academy of Sciences, Beijing 100080, People's Republic of China

\*e-mail: alg13@cam.ac.uk

Published online: 15 October 2006; doi:10.1038/nmat1758

**M**etallic glasses, now that many compositions can be made in bulk<sup>1–3</sup>, are of interest for structural applications exploiting their yield stress and strain, which are exceptionally high for metallic materials<sup>4</sup>. Their applicability is limited by their near-zero tensile ductility resulting from work-softening and shear localization. Even though metallic glasses can show extensive local plasticity, macroscopically they can effectively be brittle, and much current research is directed at improving their general plasticity. In conventional engineering materials as diverse as silicate glasses and metallic alloys, we can improve mechanical properties by the controlled introduction of compressive surface stresses<sup>5–7</sup>. Here we demonstrate that we can controllably induce such residual stresses in a bulk metallic glass, and that they improve the mechanical performance, in particular the plasticity, but that the mechanisms underlying the improvements are distinct from those operating in conventional materials.

Conventional silicate glasses, and some ceramics, can be strengthened (up to four times<sup>5</sup>) by tempering: compressive residual stresses at their surfaces suppress the cracking that leads to brittle fracture. In thermal tempering of a glass sheet, the surfaces are rapidly chilled using cold-air blasts, inducing a parabolic variation of stress through the thickness. The maximum tensile stress at the centre, roughly half the maximum compressive stress at the surface, is sufficient to give multiple fractures, desirable in safety glass<sup>6</sup>. In chemical tempering, the composition of the glass surface is altered, at high temperature, to one of lower thermal expansion coefficient<sup>6</sup>. This induces compressive stresses only in a thin surface layer; the tensile stress in the interior is small and relatively uniform. For conventional engineering alloys, surface deformation, by rolling or shot-peening, induces compressive residual stresses at the surface<sup>7</sup>. The effect is not strengthening (brittle fracture is not the failure mode), but instead increased fatigue resistance<sup>7</sup>.

In metallic glasses, residual stresses have been studied mostly because of their detrimental effect on soft-magnetic properties<sup>8,9</sup>. In bulk metallic glasses (BMGs), they have been invoked to explain difficulties in the measurement of toughness<sup>10</sup>, and are a possible threat to dimensional stability on cooling<sup>11,12</sup>. The stress profile in an as-cast BMG cylinder is of the parabolic form expected for thermal tempering of a conventional glass<sup>11</sup>. The development of residual stress by surface chilling depends on the temperature

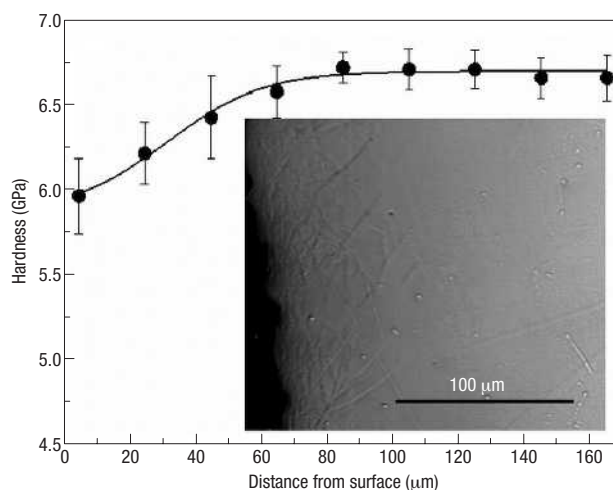


**Figure 1** Cross-section through a shot-peened layer on the surface of Zr-based bulk metallic glass. In a layer made by peening for 30 s, instrumented indentation tests show decreased hardness (data shown with standard deviation on ten measurements), and the optical micrograph (inset) shows a dense pattern of shear bands. Both methods indicate a layer thickness of 80 μm.

gradients as the sample cools through the glass transition. The thermal conductivity in metallic glasses is roughly one order of magnitude higher than in silicate glasses, and, consequently, faster chilling is required to attain significant residual stresses by thermal tempering.

Strengthening of a BMG matrix by a dispersion of particles has been attributed to tensile residual stresses in the matrix<sup>13</sup>. Otherwise, the potential beneficial effects of residual stress on mechanical properties do not seem to have been considered for BMGs. Plastic flow in metallic glasses is localized into shear bands associated with work softening<sup>14,15</sup>. As a result, the glasses show essentially zero ductility in tension and limited plasticity in compression. In bend-tests on notched bars, some metallic glasses show large values of fracture toughness, but the toughness is

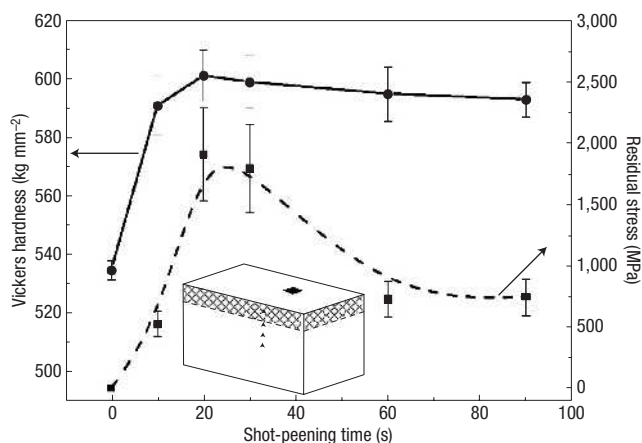


**Figure 2** Effects of shot-peening on the surface residual stress and hardness.

Vickers hardness (continuous line, data shown with standard deviation on ten measurements) of the peened surface of a Zr-based BMG, and residual stress (dashed line, estimated standard error) within the peened layer, as a function of peening time; the lines are guides for the eye. Inset: The surface indents (Vickers, represented by a black square) sample a residual stress state different from that relevant for the indents (Berkovich, represented by black triangles) in a cross-section through the peened layer (Fig. 1a).

abnormally sensitive to notch-root radius, and takes low values for sharp fatigue cracks<sup>16</sup>. The sensitivity to defects and lack of ductility provide some similarity with conventional glasses. With widespread exploitation of residual stresses in conventional glass components, it is surprising that similar effects have not been explored for BMGs.

The embrittlement of BMGs on annealing could impede the interpretation of residual stress effects. In the present work, thermal tempering, including those necessary for potential chemical tempering, were therefore avoided. Instead, the surfaces of BMGs were shot-peened, as for conventional engineering alloys<sup>7</sup>. The Zr-based BMG Vitreloy 1 was chosen, because it has been widely characterized. Shot-peening induces a typical surface roughness of 1.3  $\mu\text{m}$ . A cross-section through a peened surface, when polished and etched (Fig. 1b), shows shear bands to a depth of 80  $\mu\text{m}$ . Instrumented indentation tests (Berkovich indents typically 3.8  $\mu\text{m}$  diameter) on the cross-section show that the measured hardness decreases in the shear-banded surface layer (Fig. 1a), ultimately showing a softening of  $\sim 10\%$ , similar to that observed by Bei *et al.*<sup>15</sup> in a Zr-based BMG heavily deformed by uniaxial compression. Microhardness tests (Vickers indents, typically 84  $\mu\text{m}$  diameter) are suitable for direct characterization of the roughened, peened surfaces. As the indent diameter is similar to the peened layer depth, the hardness values obtained are not representative of the peened layer alone<sup>17</sup>. The difference in indentation techniques precludes direct comparison of the hardness values measured on the surface and on the cross-section (Fig. 2b). Nevertheless, given the data in Fig. 1a, the increase in measured surface hardness (Fig. 2a) cannot be attributed to work hardening.

Instead, the variation of surface hardness is correlated with the compressive residual stress induced in the peened layer (Fig. 2a). This stress is evident from the convex curvature developed on the peened face on a BMG plate. We calculate the stress values in Fig. 2a from measured curvatures, on the assumption of a uniform biaxial stress in a peened layer 80  $\mu\text{m}$  thick. The maximum stress, reached after peening for 20–30 s, is  $1.9 \pm 0.4$  GPa, similar to the uniaxial yield stress,  $\sigma_y = 1.8$  GPa (ref. 1), of Vitreloy 1. Applying the von Mises yield criterion (without modification for any rise

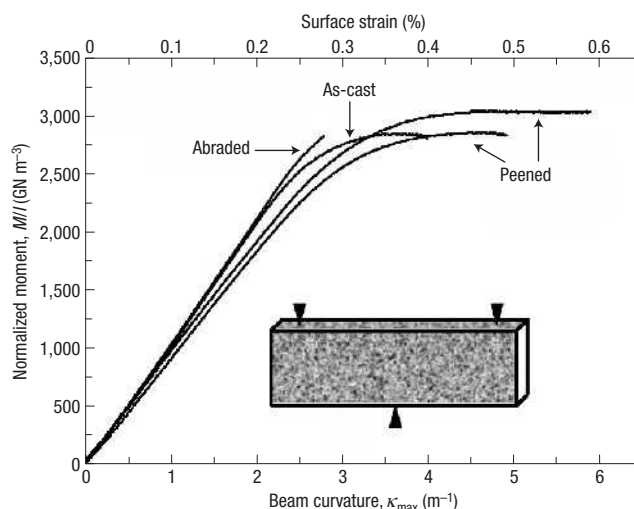


**Figure 3** Effects of surface treatments on plasticity in three-point bending.

The data are for normalized bending moment and curvature at the beam centre (that is the maximum values). An as-cast sample is compared with those with treated surfaces, shaded in the inset: one abraded and two peened samples.

of  $\sigma_y$  with pressure<sup>18</sup>), the maximum principal stress under elastic biaxial compression would be  $\sigma_y$ . The decrease in residual stress at longer peening times can be attributed to reduction of  $\sigma_y$  in heavily deformed material and to stress relaxation resulting from the heating induced by peening.

The effects of residual stress on indentation hardness tests have been extensively studied, not least because the tests could provide a convenient way to measure the stress state<sup>17,19,20</sup>. The effects are complex<sup>20</sup>, depending on the ratio of Young's modulus  $E$  to  $\sigma_y$ . In comparison with engineering alloys, metallic glasses have low values of  $E/\sigma_y$  (for Vitreloy 1,  $E/\sigma_y \approx 50$ ) (refs 1,3), and, for such materials, Chen *et al.*<sup>20</sup> show that a biaxial compressive stress in the surface leads to a smaller plastic zone underneath the indenter, to more pile-up and to increased hardness. Indentation tests on the cross-section of a peened layer (Fig. 1a) are affected differently because the residual stress state in the plane of the section is not biaxial, with a zero value for the principal stress normal to the original surface (Fig. 2b). In both cases there are competing trends: softening by introduction of shear bands and hardening by residual stress.

Three-point bend tests were conducted on simple (unnotched) BMG beams (Fig. 3a). As-cast beams without surface treatment start to yield at a strain (on top and bottom faces of the beam) of  $\sim 0.25\%$ . They then show a surface plastic strain of  $\sim 0.15\%$  before fracture. Figure 3a also shows results from beams with treated surfaces (all except the ends, as shown by the shading in Fig. 3b). A beam abraded to have surface roughness of  $\sim 0.8$   $\mu\text{m}$  fails with hardly any plastic flow, demonstrating clearly the sensitivity of BMGs to surface flaws. Beams with peened surfaces show a smeared onset of yielding and increased plastic surface strain, up to 0.25–0.35%, before failure. The roughening induced by peening might have reduced the plasticity, but clearly this is not the predominant effect.

Conventional silicate glasses fail by brittle fracture, usually initiated at surface flaws. Tempering of these glasses effectively stifles crack opening at the surface, and greatly increases strength in bending. This effect is not seen for the metallic glasses—evidence that their failure mechanism is quite different. The end of the elastic

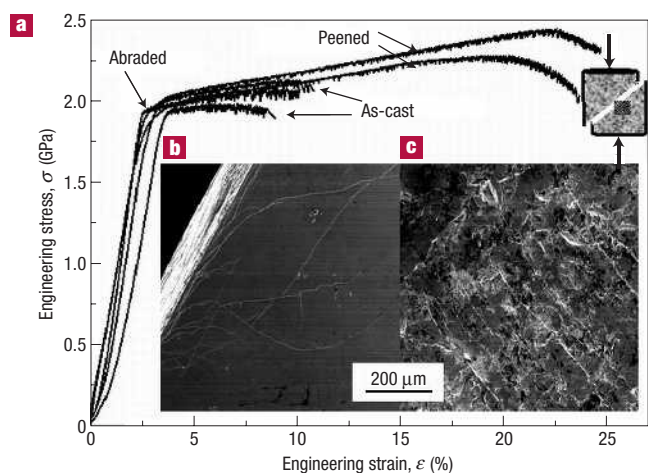


**Figure 4** Effects of surface treatments on plasticity in uniaxial compression. **a**, Two as-cast samples are compared with those with treated surfaces: one abraded, and two peened samples. **b, c**, Scanning electron micrographs of areas (shaded in the inset to **a**) close to the fracture surface show that shear-banding is sporadic in an as-cast sample (**b**), but uniformly distributed in a peened sample (**c**).

range for metallic glasses is governed by the onset of plastic flow rather than cracking. The onset of plastic flow must be facilitated, on the concave surface of the beam, by the compressive stress, and, on both concave and convex surfaces, by the shear-band initiation, induced by the peening. The greater plastic strain shown by the peened samples follows directly from the suppression of cracking by the compressive residual stress on the convex surface of the beam. That the loading necessary to maintain plastic flow is not raised by peening suggests that yielding near the convex surface is not suppressed. A possible explanation is that yielding is readily initiated underneath the compressive surface, presumably from shear bands in the peened layer. Pre-existing shear bands are favoured locations for resumed flow<sup>21</sup>.

Compression tests on rod-shaped samples (Fig. 4a) show only a small effect of abrasion; surface flaws are not important in compression. The effects of peening are dramatic, however, with the compressive plasticity increased from the average 6%, maximum 7%, in as-cast samples to average 11%, maximum 22%, in peened samples. The compressive residual stress in peened samples, combined with the pre-existing shear bands in the surface, must lead to more bands with smaller shear on each, facilitating general continuing plasticity, rather than premature failure on a few dominant shear bands<sup>22</sup>. Direct evidence for more uniform deformation in peened samples comes from comparison of the shear-band patterns developed on compression of as-cast (Fig. 4b) and peened (Fig. 4c) samples. This is consistent with the stress-strain curves for peened samples (Fig. 4a), which appear to show smaller serrations than for as-cast samples at the same strain.

In conventional materials engineering, by tempering of silicate glasses or peening of alloys, compressive residual stresses in surfaces are exploited to improve component performance. The present work shows that, by the simple method of shot-peening, BMGs too can benefit from residual stresses. Peened BMGs show increased plasticity in bending and in compression, through a combination of reduced likelihood of surface cracking and more uniform deformation induced by a high population of pre-existing shear bands, a combination of mechanisms distinct from any found in conventional engineering materials. Compressive residual stresses at surfaces constrain plastic deformation; the resulting apparent

hardening suggests that reports of work-hardening in BMGs<sup>23,24</sup> should be interpreted with care.

## METHODS

The BMG Vitreloy 1 (a trademark of Liquidmetal Technologies, Lake Forest, California) has a nominal (at.%) composition  $\text{Zr}_{41.25}\text{Ti}_{13.75}\text{Ni}_{10}\text{Cu}_{12.5}\text{Be}_{22.5}$ . Constituent elements (purity better than 99.9% by weight) were arc-melted together and then cast into 2.0-mm-diameter rods or 1.0-mm-thick plates using water-cooled copper moulds under purified argon atmosphere. The amorphousness of the samples was verified using standard techniques of X-ray diffraction (XRD) and differential scanning calorimetry. Rectangular cross-section bars, for measuring the effects of shot-peening on effective hardness, were cut from the as-cast plates using a diamond saw to nominal dimensions  $1.0 \times 5.0 \times 10 \text{ mm}^3$ . Shot-peening was carried out in Guyson 41 d.c. equipment with air pressure of 7.0 bar and a charge of 300–400  $\mu\text{m}$  diameter fused-silica beads or 100  $\mu\text{m}$  silica sand (bead fragments). The surface roughness of peened samples was measured using a Wyko RST optical profilometer, and is characterized as the arithmetical mean deviation ( $R_a$ ). Based on the results in Fig. 2, a peening time of 30 s was chosen for the other treatments; this gives significant hardening with a uniform topography.

Optical metallography on cross-sections used 1  $\mu\text{m}$  diamond paste as the final polishing step, followed by electroetching at 5 V in a solution of 33 vol% dilute nitric acid in methanol. Imaging used differential interference contrast in a Zeiss Axiotech 25DH microscope with  $\times 200$  objective. Scanning electron microscopy was on a JEOL 6340 FEGSEM operated at 10 kV.

Instrumented-indentation measurements were made on cross-sections of peened samples, cut and then polished with a final grade of 100 nm diamond film. A NanoTest 600 instrument was used, with Berkovich indenter, maximum load 50 mN, and loading rate  $1 \text{ mN s}^{-1}$ . Before Vickers hardness tests the roughened peened surfaces were polished (2,500 grit, then 1  $\mu\text{m}$  diamond). Vickers hardness was measured under 2 kg load with 10 s dwell time in a Mitutoyo MVK-H2 testing machine. For both types of indentation, the hardness values quoted are the averages of ten measurements each.

Samples for three-point bend tests were cut to dimensions 2 mm high, 1 mm wide and 30 mm long by electro-discharge machining. The tests were carried out using a table-top screw-driven machine (Hounsfield model H5KS) with spanning distance 25 mm at loading rate  $0.05 \text{ mm min}^{-1}$ . To permit direct comparison of beams with slightly different cross-sections, the data (Fig. 3) are plotted in terms of a bending moment  $M$  normalized with respect to the second moment of area  $I$ , as a function of the beam curvature  $\kappa$ .

Rods for uniaxial compression tests were cut and polished to  $\sim 3 \text{ mm}$  length, taking care that the end faces are accurately perpendicular to the rod axis. The effects of aspect ratio (height/diameter) on compression tests have been extensively studied for a Zr-based BMG<sup>25</sup>. On the basis of these results, an aspect ratio of 1.5 is chosen for the present work, to be sensitive to changes in intrinsic plasticity. The tests were done on an Instron 5567 screw-driven machine at loading rate  $5.6 \times 10^{-4} \text{ m s}^{-1}$ . Displacements were measured using an Instron strain-gauge extensometer. For as-cast and peened samples, the plastic strain varied widely, as expected for a defect-sensitive material. The averages quoted are for six tests. The curves in Fig. 4 compare maximum strains for the as-cast and peened conditions, corresponding to relatively defect-free and uniformly peened samples.

We estimated the residual stress in peened layers from curvature measurements on a BMG plate ( $1.0 \times 10 \times 35 \text{ mm}^3$ ) peened on one face. The stress in peened layers is assumed to be uniform (set by the elastic limit and independent of distance from the surface), and the deformation of the material beneath the peened layer is taken to be purely elastic, a reasonable assumption, given that the peened layer is work-softened relative to the bulk. We used a Ferranti profilometer with a tip scanning speed of  $0.6 \text{ mm s}^{-1}$  to obtain 3D co-ordinates for four line-scans parallel to the length of the unpeened face. The data were analysed to extract a best value for a cylindrical curvature. The maximum curvature measured was  $8.5 \pm 0.3 \text{ m}^{-1}$ . By comparing curvatures before and after peening, the principal residual stress  $\sigma$  in the plane of the peened surface was calculated using an equation due to Atkinson and assessed by Klein<sup>26</sup>:

$$\sigma = \frac{E_s t_s^3 \kappa}{6t_c^2 (1 - \nu_s) [1 + (t_s/t_c)]} \quad (1)$$

where  $E_s$  is the Young modulus of the substrate (that is undeformed) metallic glass, taken to be 95 GPa (refs 1,3);  $t_s$  is the thickness of the undeformed metallic glass;  $\kappa$  is the curvature ( $=1/R$ , where  $R$  is the measured radius of curvature);  $\nu_s$  is the Poisson ratio of the undeformed metallic glass, taken to be 0.353 (refs 1,3), and  $t_c$  is the thickness of the coating (that is the peened layer). Equation (1) is used rather than the Stoney equation<sup>26</sup> because the thickness of the peened layer ( $t_c = 80 \mu\text{m}$ ) is a significant fraction of the thickness of the undeformed bulk plate ( $t_s = 920 \mu\text{m}$ ). The uncertainty in the calculated residual stress values is large ( $\pm 20\%$ ) largely because of the uncertainty in  $t_s$  and  $t_c$ .

Received 7 June 2006; accepted 13 September 2006; published 15 October 2006.

## References

- Johnson, W. L. Bulk glass-forming metallic alloys: science and technology. *Mater. Res. Soc. Bull.* **24**, 42–56 (1999).
- Inoue, A. Stabilization of metallic supercooled liquid and bulk amorphous alloys. *Acta Mater.* **48**, 279–306 (2000).
- Wang, W. H., Dong, C. & Shek, C. H. Bulk metallic glasses. *Mater. Sci. Eng. R* **44**, 45–89 (2004).
- Ashby, M. F. & Greer, A. L. Metallic glasses as structural materials. *Scr. Mater.* **54**, 321–326 (2006).
- Gardon, R. in *Elasticity and Strength in Glasses* (eds Uhlmann, D. & Kreidl, N. J.) 145–216 (Glass: Science and Technology, Vol. 5, Academic, New York, 1980).
- Zarzycki, J. *Glasses and the Vitreous State* 398–404 (Cambridge Univ. Press, Cambridge, 1991).
- Evans, E. B. in *Encyclopedia of Materials Science and Engineering* Vol. 6, (ed. Bever, M. B.) 4187–4188 (Pergamon, Oxford, 1986).
- Okazaki, Y. Loss deterioration in amorphous cores for distribution transformers. *J. Magn. Magn. Mater.* **160**, 217–222 (1996).
- Tejedor, M., Garcia, J. A., Carrizo, J., Elbaile, L. & Santos, J. D. Effect of residual stresses and surface roughness on coercive force in amorphous alloys. *J. Appl. Phys.* **91**, 8435–8437 (2002).
- Ritchie, R. O., Schroeder, V. & Gilbert, C. J. Fracture, fatigue and environmentally-assisted failure of a Zr-based bulk amorphous metal. *Intermetallics* **8**, 469–475 (2000).
- Aydiner, C. C. & Üstündağ, E. Residual stresses in a bulk metallic glass cylinder induced by thermal tempering. *Mech. Mater.* **37**, 201–212 (2005).
- Aydiner, C. C. *et al.* Residual stresses in a bulk metallic glass—stainless steel composite. *Mater. Sci. Eng. A* **399**, 107–113 (2005).
- Kim, Y. C., Fleury, E., Lee, J. C. & Kim, D. H. Origin of the simultaneous improvement of strength and plasticity in Ti-based bulk metallic glass matrix composites. *J. Mater. Res.* **20**, 2474–2479 (2005).
- Spaepen, F. A microscopic mechanism for steady state inhomogeneous flow in metallic glasses. *Acta Metall.* **25**, 407–415 (1977).

- Bei, H., Xie, S. & George, E. P. Softening caused by profuse shear banding in a bulk metallic glass. *Phys. Rev. Lett.* **96**, 105503 (2006).
- Lowhaphandu, P. & Lewandowski, J. J. Fracture toughness and notched toughness of bulk amorphous alloy: Zr-Ti-Ni-Cu-Be. *Scr. Mater.* **38**, 1811–1817 (1998).
- Suresh, S. & Giannakopoulos, A.E. A new method for estimating residual stresses by instrumented sharp indentation. *Acta Mater.* **46**, 5755–5767 (1998).
- Lowhaphandu, P., Montgomery, S. L. & Lewandowski, J. J. Effects of superimposed hydrostatic pressure on flow and fracture of a Zr-Ti-Ni-Cu-Be bulk amorphous alloy. *Scr. Mater.* **41**, 19–24 (1999).
- Carlsson, S. & Larsson, P.-L. On the determination of residual stress and strain fields by sharp indentation testing. Part I: Theoretical and numerical analyses. *Acta Mater.* **49**, 2179–2191 (2001).
- Chen, X., Yan, J. & Carlsson, A. M. On the determination of residual stress and mechanical properties by indentation. *Mater. Sci. Eng. A* **416**, 139–149 (2006).
- Krishnanand, K. D. & Cahn, R. W. Recovery from plastic deformation in a Ni/Nb alloy glass. *Scr. Metall.* **9**, 1259–1261 (1975).
- Conner, R. D., Johnson, W. L., Paton, N. E. & Nix, W. D. Shear bands and cracking of metallic glass plates in bending. *J. Appl. Phys.* **94**, 904–911 (2003).
- Das, J. *et al.* Work-hardenable ductile bulk metallic glass. *Phys. Rev. Lett.* **94**, 205501 (2005).
- Yang, B., Riester, L. & Nieh, T. G. Strain hardening and recovery in a bulk metallic glass under nanoindentation. *Scr. Mater.* **54**, 1277–1280 (2006).
- Zhang, Z. F., Zhang, H., Pan, X. F., Das, J. & Eckert, J. Effect of aspect ratio on the compressive deformation and fracture behaviour of Zr-based bulk metallic glass. *Phil. Mag. Lett.* **85**, 513–521 (2005).
- Klein, C. A. How accurate are Stoney's equation and recent modifications. *J. Appl. Phys.* **88**, 5487–5489 (2000).

## Acknowledgements

Y.Z. acknowledges support from Trinity College Cambridge and the Schlumberger Cambridge Trust, W.H.W. from the National Science Foundation of China and A.L.G. from the European Commission under MCRTN contract 'Ductile bulk metallic glass composites'. Correspondence and requests for materials should be addressed to A.L.G.

## Author contributions

Y.Z. was responsible for the experimental work, W.H.W. for supervising sample preparation, A.L.G. for supervising structural characterization and mechanical testing, and all authors for interpretation of results.

## Competing financial interests

The authors declare that they have no competing financial interests.

Reprints and permission information is available online at <http://npg.nature.com/reprintsandpermissions/>